ZOOLOGICAL SCIENCE **15**: 447–453 (1998)

Immunolocalization of Vacuolar-Type H^+-ATPase in the Yolk-Sac Membrane of Tilapia (*Oreochromis mossambicus*) Larvae

Junya Hiroi[1,2], Toyoji Kaneko[2], Katsuhisa Uchida[2], Sanae Hasegawa[2] and Masaru Tanaka[1]*

[1]*Division of Applied Biosciences, Graduate School of Agriculture, Kyoto University, Kitashirakawa-Oiwakecho, Sakyo, Kyoto 606-8502, Japan*
[2]*Ocean Research Institute, University of Tokyo, Minamidai, Nakano, Tokyo 164-8639, Japan*

ABSTRACT—To investigate the involvement of the yolk-sac membrane in ion absorption, developmental changes in whole-body cation contents, cellular localization of vacuolar-type H^+-ATPase (V-ATPase), and size and density of pavement and chloride cells in the yolk-sac membrane were examined in tilapia (*Oreochromis mossambicus*) larvae in fresh water (FW) and those transferred to seawater (SW) at 2 days before hatching (day –2). The whole-body content of Na^+ in embryos and larvae adapted to both FW and SW increased constantly from day –2 to day 10, although they were not fed through the experiment. The yolk-sac membrane of FW larvae at days 0 and 2 showed V-ATPase immunoreactivity in pavement cells, but not in chloride cells. No positive immunoreactivity was detected in SW larvae. Whole-mount immunocytochemistry showed that some pavement cells were intensively immunoreactive, whereas others were less or not immunoreactive. Electron-microscopic immunocytochemistry revealed that V-ATPase immunoreactivity was present in the apical regions of pavement cells in FW larvae, especially in their ridges. The pavement cells in FW larvae were significantly smaller in size but higher in density than those in SW. These results suggest that pavement cells are the site of active Na^+ uptake in exchange for H^+ secretion through V-ATPase in FW-adapted tilapia during early life stages.

INTRODUCTION

Freshwater (FW) teleosts take up ions from dilute environments across the gill epithelium, compensating for the constant loss of ions by diffusion (Lin and Randall, 1995; Goss *et al*., 1995; Flik *et al*., 1995). It is suggested that the branchial Na^+ uptake occurs through a Na^+ channel electrically coupled with a vacuolar-type H^+-ATPase (V-ATPase), which generates a favorable electrochemical gradient for passive electrodiffusion of Na^+ through a Na^+ channel (Lin and Randall, 1995). Previous studies using rainbow trout (*Oncorhynchus mykiss*) gills have suggested that V-ATPase immunoreactivity is distributed in both chloride and pavement cells (Lin *et al*., 1994) or in pavement cells (Sullivan *et al*., 1995). However, cellular localization of V-ATPase and its involvement in Na^+ uptake are still controversial in teleosts.

Embryos and larvae without functional gills can also maintain internal ion concentrations (Alderdice, 1988). The gills occupy a large proportion of the body surface in adult form of fish, whereas the epithelia covering the body and yolk are the major part of the body surface in early life stages. The outermost layer of these epithelia consists of pavement cells and, to a less extent, chloride cells. Thus, these cell types in the body skin and yolk-sac membrane could be the site of ion regulation in embryos and yolk-sac larvae, which lack functional gills. In fact, chloride cells in the body skin and yolk-sac membrane have been suggested to be the site of salt secretion in seawater (SW)-adapted embryos and larvae of several teleosts (Shelbourne, 1957; Lasker and Threadgold, 1968; Hwang and Hirano, 1985; Alderdice, 1988; Hwang, 1989, 1990; Ayson *et al*., 1994; Kaneko *et al*., 1995; Shiraishi *et al*., 1997). However, little information is available on ion uptake mechanisms in FW-adapted embryos and larvae.

In the present study, we examined changes in whole-body cation contents during the early development of euryhaline tilapia (*Oreochromis mossambicus*) in FW and those adapted to SW. To explore the possible involvement of the yolk-sac membrane in ion absorption, cellular localization of V-ATPase was also examined in FW and SW fish, concomitant with morphometrical analyses of pavement and chloride cells. Our findings suggest that Na^+ uptake occurs in pavement cells of the yolk-sac membrane in FW-adapted tilapia during early life stages, when functional gills are lacking.

* Corresponding author: Tel. +81-75-753-6220; FAX. +81-75-753-6229.

MATERIALS AND METHODS

Fish

Mature tilapia (*Oreochromis mossambicus*) were maintained in tanks with recirculating FW (Na^+, 0.74 mM; Ca^{2+}, 0.54 mM; Mg^{2+}, 0.26 mM) at 25°C. Fertilized eggs were obtained from the mouth of brooding females at 3 days after fertilization (2 days before hatching, day –2). They were separated into two groups: half of the embryos were maintained in FW, and the other half were transferred directly to SW (Na^+, 490 mM; Ca^{2+}, 16 mM; Mg^{2+}, 66 mM) at day –2. They were further incubated in a 5-l plastic tank containing FW or SW at 25°C. Water was gently agitated with aeration and renewed every other day. Tilapia embryos usually hatched after 5 days' incubation at 25°C, and yolk absorption was completed by 10 days after hatching. Larvae were not fed during the experiment.

Whole-body cation contents

FW embryos at day –2 and FW and SW larvae at days 0, 2, 5 and 10 were rinsed with distilled water, weighed and preserved at –20°C. The chorion of embryos was torn off with sharp-pointed forceps. Whole-body cation contents were measured following the method of Uchida *et al.* (1993) with some modifications. Each sample was dissolved with 500 µl of a mixture of nitric acid and perchloric acid (11:2). The concentrations of Na^+, Ca^{2+} and Mg^{2+} were measured with an atomic absorption spectrophotometer (Hitachi 180-50, Japan).

Semi-thin section immunocytochemistry

FW and SW larvae at days 0 and 2 were fixed in 4% paraformaldehyde in 0.1 M phosphate buffer (PB, pH 7.4) for 20 hr at 4°C, dehydrated through graded ethanols, transferred to propylene oxide and embedded in Spurr's resin. Cross sections were cut at 1 µm thickness with glass knives, and mounted on slides coated with Biobond adhesive (British BioCell, UK). The sections were treated with saturated potassium hydroxide in ethanol for 10 min to remove the resin, and then subjected to immunocytochemical staining for V-ATPase based on the silver enhancement method (Springall *et al.*, 1984). The sections were incubated sequentially with: 1) 2% normal goat serum in 0.01 M phosphate-buffered saline (PBS, pH 7.2) for 30 min, 2) rabbit anti-V-ATPase diluted 1:2000 for 20 hr at 4°C, and 3) goat anti-rabbit IgG conjugated with 5 nm-immunogold (British BioCell, UK) diluted 1:100 for 2 hr. The immunoreaction was visualized by treating the sections with the silver enhancing reagent (British BioCell, UK) for 10 min at 22°C. The antiserum was diluted with PBS containing 2% normal goat serum, 0.1% bovine serum albumin and 0.01% sodium azide (BPBS). The sections were then washed with distilled water, coverslipped with distilled water, and examined with a microscope equipped with a Nomarski's differential interference contrast (DIC) device. Mounting medium was not used because it reduced the contrast of DIC images.

Whole-mount immunocytochemistry

After FW and SW larvae at day 2 were fixed in 4% paraformaldehyde in PB for 30 min, the yolk sac was incised and the yolk was carefully scraped out with sharp-pointed forceps. Larvae were further fixed for 6 hr and preserved in 70% ethanol. Whole-mount immunocytochemistry based on the avidin-biotin-peroxidase complex (ABC) method (Hsu *et al.*, 1981) with commercial reagents (Vectastain ABC kit, Vector Laboratories, USA) was carried out following the method of Ohtani *et al.* (1989). After treatment with 0.1% sodium cyanoborohydride in PBS for 1 hr, the samples were incubated sequentially with: 1) rabbit anti-V-ATPase diluted 1:500 for 20 hr at 4°C, 2) biotinylated goat anti-rabbit IgG for 20 hr at 4°C, 3) ABC reagent for 20 hr at 4°C, and 4) 0.03% 4-Cl-1-naphthol in 0.05 M Tris-HCl buffer (pH 7.6) containing 0.003% hydrogen peroxide for 20 min. The antiserum was diluted with PBS containing 0.05% Triton X-100, 10% normal goat serum, 0.1% bovine serum albumin and 0.01% sodium azide. The yolk-sac membrane was then removed, mounted on a slide with glycerin, and examined with a microscope equipped with a Nomarski's DIC device.

Electron-microscopic immunocytochemistry

FW and SW larvae at day 2 were fixed in 2% paraformaldehyde-0.2% glutaraldehyde in PB for 3 hr at 4°C and embedded in Spurr's resin. Ultra-thin sections were cut with a diamond knife and mounted on nickel grids. The sections were incubated sequentially with: 1) BPBS for 5 min, 2) rabbit anti-V-ATPase diluted 1:1000 with BPBS for 2 hr, and 3) goat anti-rabbit IgG conjugated with 10 nm-immunogold (British BioCell, UK) diluted 1:50 with PBS for 1hr. All procedures were performed at room temperature. The sections were then stained with uranyl acetate (10 min) and lead citrate (1 min), and examined with a transmission electron microscope (Hitachi H-7100, Japan).

Antiserum

The polyclonal antibody used here was raised in a rabbit against a V-ATPase 72 kDa subunit A isolated from chromaffin granule membranes in bovine adrenal medulla (Moriyama and Yamamoto, 1995). The antiserum was kindly provided by Professor Yoshinori Moriyama, Institute of Scientific and Industrial Research, Osaka University. To confirm the specificity of the immunoreactivity, the primary antiserum was replaced with normal rabbit serum at the same dilution, which resulted in extinction of the immunoreaction.

Morphometrical analyses of pavement and chloride cell

FW and SW larvae at day 2 were fixed in the same procedure as the whole-mount immunocytochemistry, and then postfixed in 1% osmium tetroxide in PB for 1 hr. After the larvae were washed with distilled water, the yolk-sac membrane was removed, mounted on a slide with distilled water, and examined with a microscope equipped with a Nomarski's DIC device. The images of 10 fields, corresponding to 0.274 mm^2, from each individual were digitized with a CCD video camera (Victor, Japan) and an image processor (ARGUS 20, Hamamatsu photonics, Japan), and the area and density of pavement and chloride cells were measured on an Apple Macintosh computer using the public domain NIH Image program (available on the Internet at http://rsb.info.nih.gov/nih-image/).

Statistics

Significant differences in whole-body cation contents were examined by two-way ANOVA with repetition (time x environment) followed by the Scheffe's F test. Before analysis, data displaying heterogeneity of variance were log-transformed. Significant differences in size and density of pavement and chloride cells between FW and SW groups were tested by the Kolmogorov-Smirnov test and the Mann-Whitney U test, respectively.

RESULTS

Whole-body cation contents

Developmental changes in whole-body cation contents are shown in Fig. 1. The Na^+ content of embryos and larvae adapted to both FW and SW increased constantly from day –2 to day 10. The whole-body Ca^{2+} content of both groups kept a constant level before hatching, doubled at day 2, and increased rapidly thereafter. In contrast, the Mg^{2+} content of both groups showed no significant change during the experiment. There were no significant differences in the three cation contents between FW and SW.

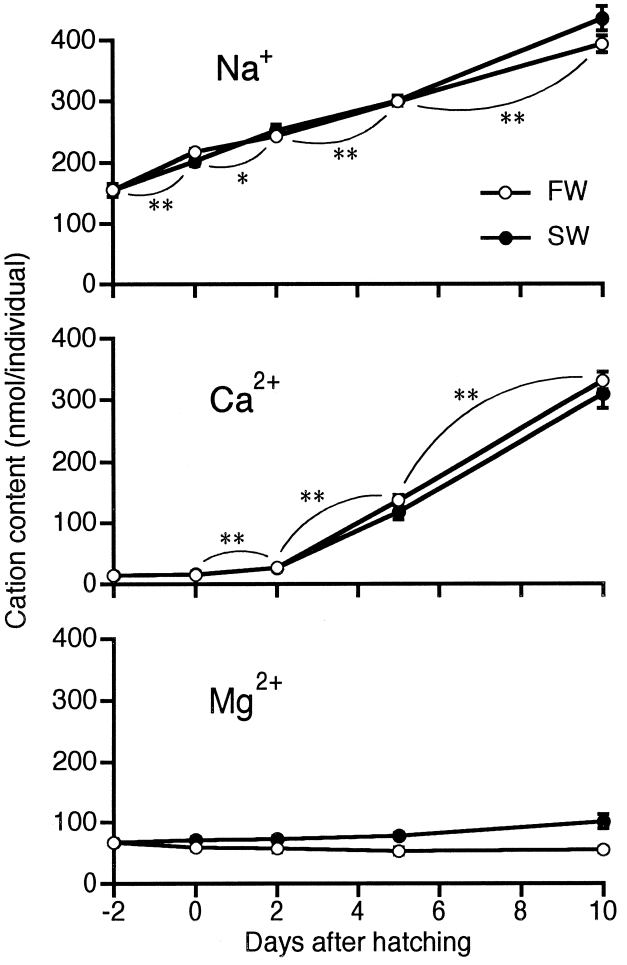

Fig. 1. Developmental changes in whole-body cation contents. Vertical bars represent standard errors of the means of 10 individuals. Asterisks indicate significant differences by the Scheffe's F test. $^{*}p < 0.01$, $^{**}p < 0.001$.

Semi-thin section and whole-mount immunocytochemistry

In the semi-thin section immunocytochemistry, V-ATPase immunoreactivity was detected in the yolk-sac membrane of FW larvae at days 0 and 2, whereas the positive immunoreactivity was not detectable in SW larvae at days 0 and 2 (Fig. 2). The DIC images allowed to distinguish between pavement and chloride cells. Cone-like shaped chloride cells were in contact with the basal membrane on the serosal side, and with external environments on their apical membrane forming a pit. In FW larvae, V-ATPase immunoreactivity was restricted to pavement cells, and was not detected in chloride cells (Fig. 2A). However, V-ATPase immunoreactivity was not observed in all pavement cells in FW larvae, which was further confirmed by the whole-mount immunocytochemistry. Figure 3 shows whole-mount preparations of the yolk-sac membrane of FW and SW larvae at day 2, stained with anti-V-ATPase. Some pavement cells in FW larvae showed strong immunoreactivity, whereas others showed little or no immunoreactivity (Fig. 3A). Chloride cells, readily distinguishable from pavement cells by changing the focus, showed no immunoreactivity. In addition, no positive immunoreactivity was detected in pavement and chloride cells of SW larvae (Fig. 3B).

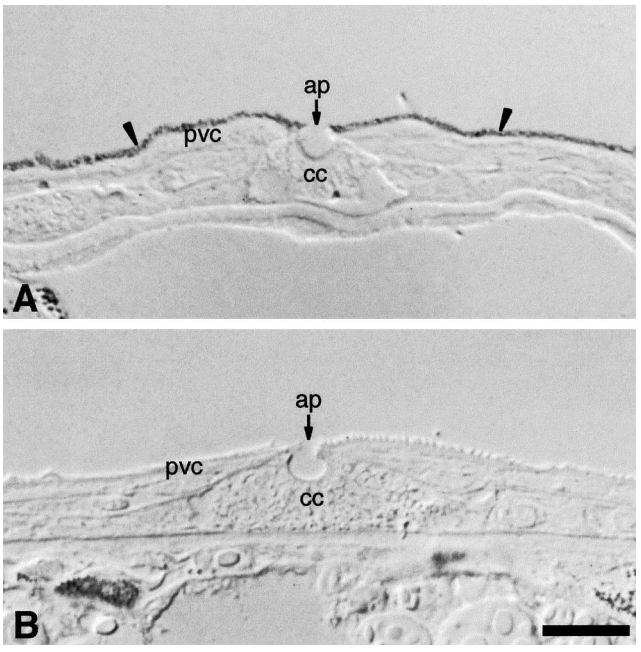

Fig. 2. DIC micrographs of the yolk-sac membrane stained with anti-V-ATPase in larvae (day 2) adapted to FW (**A**) and SW (**B**). V-ATPase immunoreactivity (arrowheads) is detectable in pavement cells (pvc), but not in chloride cells (cc), in FW larvae. Both pavement and chloride cells are immunonegative in SW larvae. ap, apical pit of chloride cells. Bar: 10 μm.

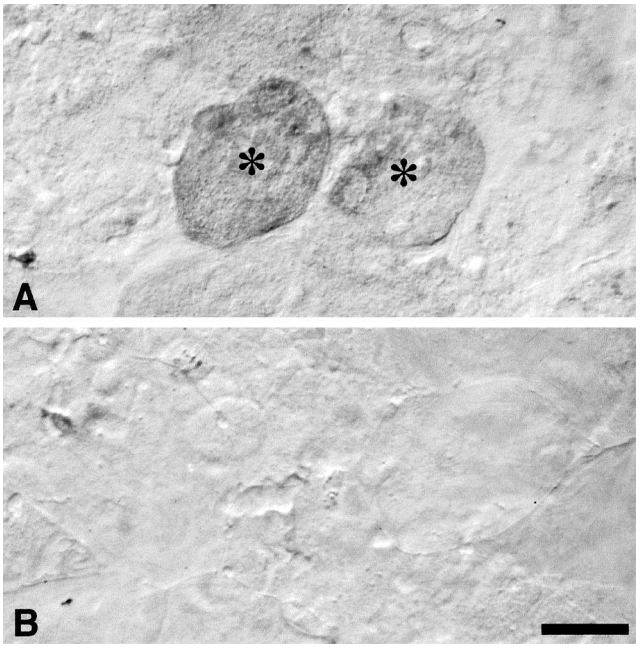

Fig. 3. Whole-mount preparations of the yolk-sac membrane stained with anti-V-ATPase in larvae (day 2) adapted to FW (**A**) and SW (**B**). Some pavement cells are immunoreactive (asterisks) in FW larvae, while no immunoreactivity is detectable in SW larvae. Bar: 20 μm.

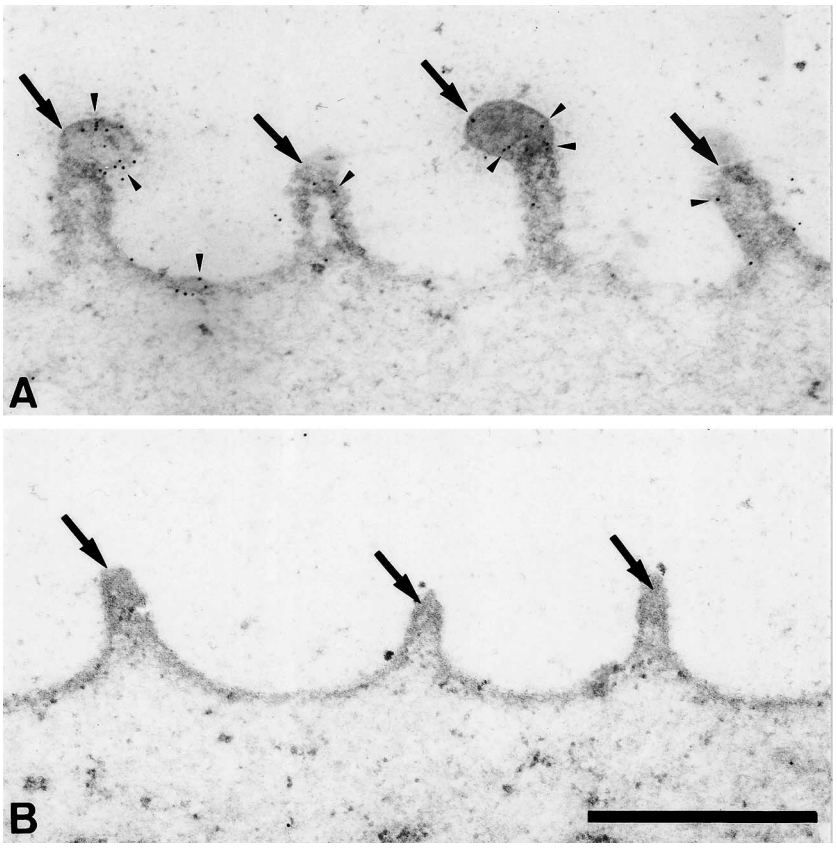

Fig. 4. Transmission-electron micrographs of pavement cells in the yolk-sac membrane stained with anti-V-ATPase in larvae (day 2) adapted to FW (**A**) and SW (**B**). Immunogold labeling (arrowheads) is mainly located in the apical regions of pavement cells, especially in the ridge structures (arrows), in FW larvae. Pavement cells in SW larvae are immunonegative. Bar: 1 μm.

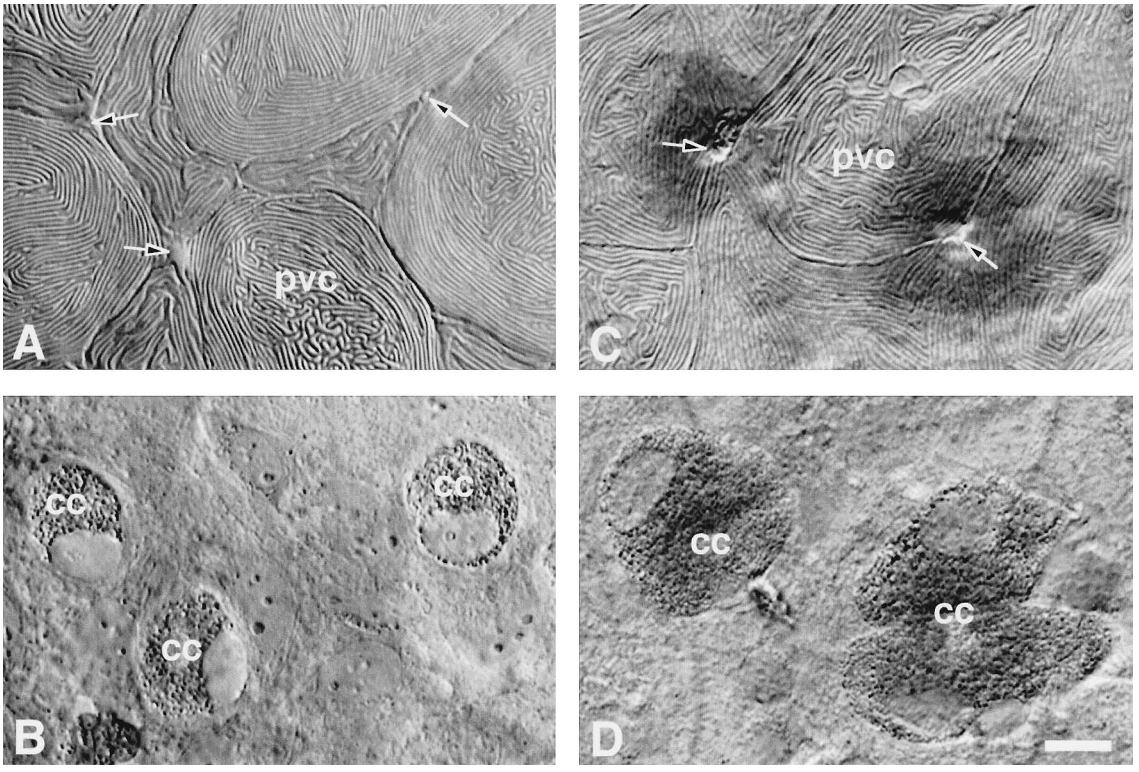

Fig. 5. DIC micrographs of whole-mount preparations of the yolk-sac membrane in larvae (day 2) adapted to FW (**A**, **B**) and SW (**C**, **D**). The ridge structures of pavement cells (pvc) and apical pits (arrows) of chloride cells (cc) are observable on the surface (**A**, **C**), while the underlying chloride cells are in focus on a deeper plane (**B**, **D**) of the same specimens. Bar: 10 μm.

Electron-microscopic immunocytochemistry

Figure 4 shows transmission-electron micrographs of the yolk-sac membrane of FW and SW larvae at day 2. In FW larvae, V-ATPase immunogold labeling was present in the apical regions of the pavement cells, especially in the ridge structures (Fig. 4A). In accordance with the light-microscopic observations, no immunogold labeling was detected in SW larvae (Fig. 4B).

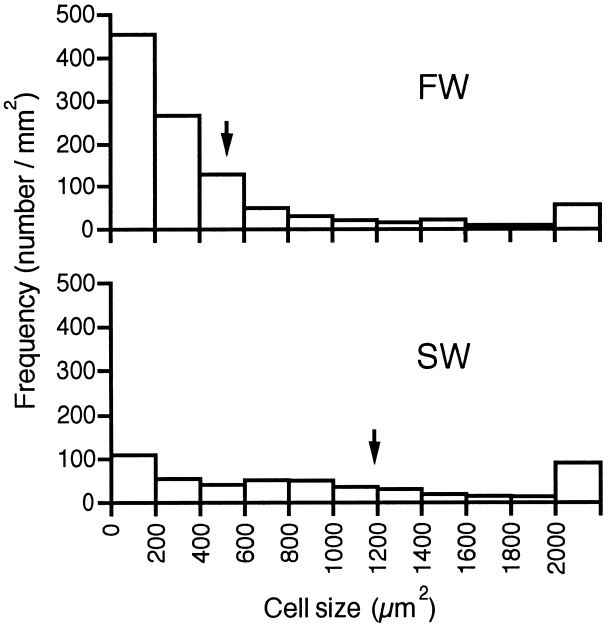

Fig. 6. Size-frequency distributions of pavement cells in the yolk-sac membrane of larvae (day 2) adapted to FW and SW. Data obtained from 4 individuals were combined in each group. Arrows indicate the means.

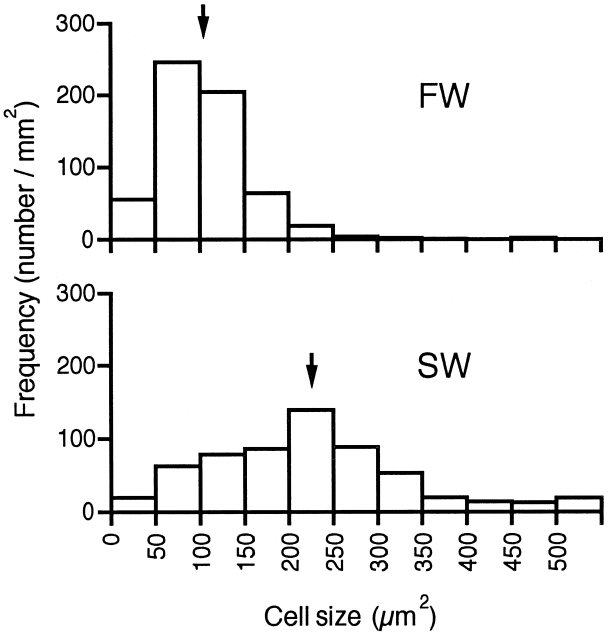

Fig. 7. Size-frequency distributions of chloride cells in the yolk-sac membrane of larvae (day 2) adapted to FW and SW. Data obtained from 4 individuals were combined in each group. Arrows indicate the means.

Size and density of pavement and chloride cells

In the whole-mount preparations of the yolk-sac membrane, the ridge structures of pavement cells and apical pits of chloride cells were clearly observed under a light microscope with a DIC device (Fig. 5A, C). In the same specimen, chloride cells were also observable beneath the pits by changing the focus (Fig. 5B, D). The pavement cells were significantly smaller ($P < 0.001$) in FW larvae than those in SW (Fig. 6). The density of pavement cells in FW larvae was 1925 ± 253 cells/mm^2 (mean ± SE, n = 4), which was significantly higher ($P < 0.05$) than those in SW (823 ± 125 cells/mm^2). The chloride cells were significantly larger ($P < 0.001$) in SW larvae than in FW larvae (Fig. 7), whereas there was no significant difference in the density of chloride cells between the two groups (FW, 462 ± 42 cells/mm^2; SW, 458 ± 50 cells/mm^2).

DISCUSSION

In the present study, a constant increase in Na^+ content was demonstrated during the early development of tilapia adapted to FW and SW. A rapid increase in Ca^{2+} content occurred at day 2, whereas Mg^{2+} content was essentially constant throughout the experiment. Hwang *et al.* (1994) observed similar increases in Na^+ and Ca^{2+} contents in FW-adapted tilapia embryos and larvae. These findings indicate that tilapia uptake Na^+ and Ca^{2+} from external environments during the early developmental stages. According to Miyazaki *et al.* (1998), FW-adapted tilapia larvae start drinking at day 2. The gills are not yet developed or not fully functional during embryonic and early larval stages (Ayson *et al.*, 1994; Li *et al.*, 1995). Taken together, Na^+ and Ca^{2+} uptakes are expected to occur mainly across the body surface during early life stages, when functional gills are lacking.

In the early life stages of tilapia, the yolk-sac membrane covering the yolk occupies a large proportion of the body surface, which contrasts with the large surface area of the gills in adult fish. The surface structure of the yolk-sac membrane is morphologically similar to that of the gills: the outermost layers of both tissues are covered with a single layer of respiratory pavement cells, and chloride cells are scattered among the pavement cells with their pits exposing to external environments. Thus, it may be reasonable to presume that the yolk-sac membrane functions as a respiratory and ion-regulating site in embryos and yolk-sac larvae in place of the gills in adult fish.

In FW fish gills, an electroneutral Na^+/H^+ exchanger in the apical membrane had been advocated as the major pathway for Na^+ uptake and H^+ secretion. However, the Na^+/H^+ exchanger model was questioned by experimental and theoretical evidence, and an alternative model incorporating an electrogenic proton pump and a conductive Na^+ channel was proposed on the analogy of other epithelia such as amphib-

ian skin (Avella and Bornancin, 1989). In this scheme, V-ATPase, an electrogenic proton pump, generates a favorable electrochemical gradient across the apical membrane and permits passive electrodiffusion of Na^+ through a Na^+ channel. The presence of V-ATPase and its mRNA has been reported in rainbow trout gills (Lin *et al.*, 1994; Sullivan *et al.*, 1995, 1996). Sullivan *et al.* (1995) have concluded that V-ATPase is present in pavement cells in rainbow trout gills. Morphological observations and X-ray microanalysis also suggest that pavement cells are the site of Na^+ uptake and H^+ secretion (Goss *et al.*, 1992, 1994; Laurent *et al.*, 1994; Morgan *et al.*, 1994). However, the occurrence of V-ATPase in chloride cells in addition to pavement cells is still controversial, partly because of the difficulty in identifying chloride cells. In the yolk-sac membrane of tilapia embryos and larvae, we were able to distinguish between pavement and chloride cells under a light microscope without difficulty, and demonstrated V-ATPase immunoreactivity only in pavement cells in FW larvae. Furthermore, the electron-microscopic immunocytochemistry revealed that V-ATPase was localized in the apical regions of pavement cells. These observations suggest that pavement cells in the yolk-sac membrane are the site of Na^+ uptake in exchange for H^+ secretion in FW-adapted tilapia larvae. This is also supported by the absence of V-ATPase immunoreactivity in SW-adapted fish.

The V-ATPase and Na^+ channel model in FW fish is based on a model established in the amphibian skin. V-ATPase is apically located in mitochondria-rich (MR) cells of the amphibian skin, which are responsible for H^+ secretion. However, MR cells are not the principal site of Na^+ transport, but granular cells are responsible for Na^+ transport (Brown and Breton, 1996; Nagel and Dörge, 1996). Since the localization of Na^+ channel was not demonstrated in the yolk-sac membrane of tilapia larvae, we are not able to conclude that V-ATPase-immunopositive pavement cells are the site of Na^+ uptake. The whole-mount immunocytochemistry revealed that pavement cells were either immunopositive or -negative to V-ATPase. It is possible that Na^+ channel might be present in a subpopulation of pavement cells which are immunonegative to V-ATPase.

The surface structures of pavement cells and apical openings of chloride cells have been observed in the yolk-sac membrane and skin of tilapia embryos and larvae by scanning-electron microscopy (Ayson *et al.*, 1994; Hwang *et al.*, 1994; Shiraishi *et al.*, 1997). Although the scanning microscopy provides information on fine surface structures of epithelia at high magnifications, chloride cells existing beneath the apical pits are not observable. In the present study, we successfully observed not only ridge structures of pavement cells and apical pits of chloride cells on the surface, but also the underlying chloride cells on a deeper plane in the same yolk-sac membrane preparations with a light microscope.

Pavement cells in the yolk-sac membrane were smaller but more numerous in FW larvae than in SW larvae. There is no difference between FW and SW in total area of the yolk-sac membrane, which is mostly covered with pavement cells. Thus, unlike chloride cells that are sparsely distributed in the yolk-sac membrane, the mean size and density of pavement cells are in inverse proportion to each other. The larger number and smaller size of pavement cells in FW than in SW might be interpreted as enhanced cellular activity in FW. It might also be possible that more frequent recruitment of newly-differentiated pavement cells in FW results in the large number and small size of these cells.

Chloride cells in the yolk-sac membrane were larger in SW larvae than in FW larvae, whereas there was no difference in density between FW and SW. These findings accord with observations by Ayson *et al.* (1994), who detected chloride cells in the yolk-sac membrane by means of DASPEI staining in FW- and SW-adapted tilapia embryos and larvae. According to Shiraishi *et al.* (1997), well-developed chloride cells in SW tilapia embryos and larvae form multicellular complexes, consisting of chloride cells and accessory cells. Chloride cells, or chloride cell complexes, in the yolk-sac membrane of SW-adapted fish are considered to be the site for salt secretion. On the other hand, the functional significance of chloride cells in the yolk-sac membrane in FW-adapted fish still remains unknown. In adult fish, gill chloride cells appear to be responsible for Ca^{2+} uptake in FW (Flik *et al.*, 1995). Compared with chloride cells in SW larvae, those in FW were small but equally numerous, suggesting that chloride cells in FW play an ion-transporting role(s) different from that in SW. The observed increase in Ca^{2+} content during the early development of FW tilapia might be due to chloride cells in the yolk-sac membrane, although no direct evidence for this issue is available at present.

In summary, V-ATPase immunoreactivity was demonstrated in pavement cells of the yolk-sac membrane of tilapia larvae adapted to FW. A constant increase in Na^+ content during the early development, the immunolocalization of V-ATPase in pavement cells, and higher density of pavement cells in FW suggest that pavement cells are the site responsible for active Na^+ uptake in exchange for H^+ secretion in FW-adapted embryos and larvae.

ACKNOWLEDGMENTS

We wish to express our gratitude to Professor Tetsuya Hirano, Ocean Research Institute, University of Tokyo, for his encouragement during the course of this study. We are grateful to Professor Yoshinori Moriyama, Institute of Scientific and Industrial Research, Osaka University, for providing the anti-V-ATPase antiserum. Thanks are also due to Dr. Takeo Kurihara, Seikai National Fisheries Research Institute, for his helpful advice on statistical analyses. This study was supported in part by Grants-in-Aid for Scientific Research from the Ministry of Education, and the Fisheries Agency, Japan. J.H. and K.U. were supported by Research Fellowships of Japan Society for Promotion of Science for Young Scientists.

REFERENCES

Alderdice DF (1988) Osmotic and ionic regulation in teleost eggs and larvae. In "Fish Physiology Vol 11A" Ed by WS Hoar, DJ Randall, Academic Press, San Diego, pp 163–251

Avella M, Bornancin M (1989) A new analysis of ammonia and sodium transport through the gills of the freshwater rainbow trout (*Salmo gairdneri*). J Exp Biol 142: 155–175

Ayson FG, Kaneko T, Hasegawa S, Hirano T (1994) Development of mitochondrion-rich cells in the yolk-sac membrane of embryos and larvae of tilapia, *Oreochromis mossambicus*, in fresh water and seawater. J Exp Zool 270: 129–135

Brown D, Breton S (1996) Mitochondria-rich, proton-secreting epithelial cells. J Exp Biol 199: 2345–2358

Flik G, Verbost PM, Wendelaar Bonga SE (1995) Calcium transport processes in fishes. In "Fish Physiology Vol 14" Ed by CM Wood, TJ Shuttleworth, Academic Press, San Diego, pp 317–342

Goss GG, Laurent P, Perry SF (1992) Evidence for a morphological component in the regulation of acid-base balance in hypercapnic catfish (*Ictalurus nebulosus*). Cell Tissue Res 268: 539–552

Goss GG, Laurent P, Perry SF (1994) Gill morphology during hypercapnia in brown bullhead (*Ictalurus nebulosus*): role of chloride cells and pavement cells in acid-base regulation. J Fish Biol 45: 705–718

Goss GG, Perry SF, Laurent P (1995) Ultrastructural and morphometric studies on ion and acid-base transport processes in freshwater fish. In "Fish Physiology Vol 14" Ed by CM Wood, TJ Shuttleworth, Academic Press, San Diego, pp 257–284

Hsu SM, Raine L, Fanger H (1981) Use of avidin-biotin complex (ABC) in immunoperoxidase techniques: a comparison between ABC and unlabeled antibody (PAP) procedures. J Histochem Cytochem 29: 577–580

Hwang PP (1989) Distribution of chloride cells in teleost larvae. J Morphol 200: 1–8

Hwang PP (1990) Salinity effects on development of chloride cells in the larvae of ayu (*Plecoglossus altivelis*). Mar Biol 107: 1–7

Hwang PP, Hirano R (1985) Effects of environmental salinity on intracellular organization and junctional structure of chloride cells in early stages of teleost development. J Exp Zool 236: 115–126

Hwang PP, Tsai YN, Tung YC (1994) Calcium balance in embryos and larvae of the freshwater-adapted teleost, *Oreochromis mossambicus*. Fish Physiol Biochem 13: 325–333

Kaneko T, Hasegawa S, Takagi Y, Tagawa M, Hirano T (1995) Hypoosmoregulatory ability of eyed-stage embryos of chum salmon. Mar Biol 122: 165–170

Lasker R, Threadgold LT (1968) "Chloride cells" in the skin of the larval sardine. Exp Cell Res 52: 582–590

Laurent P, Goss GG, Perry SF (1994) Proton pumps in fish gill pavement cells? Arch Int Physiol Biochim Biophys 102: 77–79

Li J, Eygensteyn J, Lock RAC, Verbost PM, Van Der Heijden AJH, Wendelaar Bonga SE, Flik G (1995) Branchial chloride cells in larvae and juveniles of freshwater tilapia *Oreochromis mossambicus*. J Exp Biol 198: 2177–2184

Lin H, Pfeiffer DC, Vogl AW, Pan J, Randall DJ (1994) Immunolocalization of H^+-ATPase in the gill epithelia of rainbow trout. J Exp Biol 195: 169–183

Lin H, Randall D (1995) Proton pumps in fish gills. In "Fish Physiology Vol 14" Ed by CM Wood, TJ Shuttleworth, Academic Press, San Diego, pp 229–255

Miyazaki H, Kaneko T, Hasegawa S, Hirano T (1998) Developmental changes in ion and water permeability and drinking rate during early life stages of euryhaline tilapia, *Oreochromis mossambicus*, reared in fresh water and seawater. Fish Physiol Biochem (in press)

Morgan IJ, Potts WTW, Oates K (1994) Intracellular ion concentrations in branchial epithelial cells of brown trout (*Salmo trutta* L.) determined by X-ray microanalysis. J Exp Biol 194: 139–151

Moriyama Y, Yamamoto A (1995) Microvesicles isolated from bovine pineal gland specifically accumulate L-glutamate. FEBS Lett 367: 233–236

Nagel W, Dörge A (1996) The role of mitochondria-rich cells in sodium transport across amphibian skin. Pflüers Arch / Eur J Physiol 433: 146–152

Ohtani R, Kaneko T, Kline LW, Labedz T, Tang Y, Pang PKT (1989) Localization of calcitonin gene-related peptide in the small intestine of various vertebrate species. Cell Tissue Res 258: 35–42

Shelbourne JE (1957) Site of chloride regulation in marine fish larvae. Nature 180: 920–922

Shiraishi K, Kaneko T, Hasegawa S, Hirano T (1997) Development of multicellular complexes of chloride cells in the yolk-sac membrane of tilapia (*Oreochromis mossambicus*) embryos and larvae in seawater. Cell Tissue Res 288: 583–590

Springall D, Hacker G, Grimelius L, Polak J (1984) The potential of the immuno-gold silver staining method for paraffin sections. Histochemistry 81: 603–608

Sullivan GV, Fryer JN, Perry SF (1995) Immunolocalization of proton pumps (H^+-ATPase) in pavement cells of rainbow trout gill. J Exp Biol 198: 2619–2629

Sullivan GV, Fryer JN, Perry SF (1996) Localization of mRNA for the proton pumps (H^+-ATPase) and Cl^-/HCO_3^- exchanger in the rainbow trout gill. Can J Zool 74: 2095–2103

Uchida K, Ohtani Y, Sasayama Y, Nambu H, Yoshizawa H, Akabane S, Suzuki K, Suzuki N (1993) Levels of calcium in the skin of some amphibians and possible evolutionary implications. Zool Sci 10: 819–826

(Received April 21, 1998 / Accepted May 14, 1998)